THE JOURNAL OF PHYSICAL CHEMISTRY A
A JOURNAL OF THE AMERICAN CHEMICAL SOCIETY

pubs.acs.org/JPCA

Article

A Tale of Two Tails: Rotational Spectroscopy of *N*-Ethyl Maleimide and *N*-Ethyl Succinimide

Lughnasa York, Caroline Sorrells, Chisom A. Dim, Kyle N. Crabtree, and A. O. Hernandez-Castillo*

Cite This: *J. Phys. Chem. A* 2024, 128, 5541−5547

Read Online

ACCESS | Metrics & More | Article Recommendations | Supporting Information

ABSTRACT: Broadband microwave spectra of *N*-ethyl maleimide (NEM) and *N*-ethyl succinimide (NES) have been recorded using chirped pulse Fourier transform microwave spectroscopy in the K_a-band (26.5−40 GHz). The spectra for both molecules were fit to a Watson A-reduced Hamiltonian in the I^r representation to obtain best fit experimental rotational constants (NEM: A_0 = 2143.1988(29), B_0 = 1868.7333(22), C_0 = 1082.98458(36); NES: A_0 = 2061.47756(14), B_0 = 1791.73517(12), C_0 = 1050.31263(11)), centrifugal distortion constants, and nuclear quadrupole coupling constants. While the heavy atoms of the five-membered ring of both molecules are planar, the ethyl chain has its terminal methyl group perpendicular to the ring. Along the relaxed potential energy curve for the ethyl dihedral angle (θ_1 = C(6)−C(5)−N−C(4)), the ethyl group experiences significant steric strain when it is in the plane of the ring, associated with the interaction of the ethyl group with the two carbonyl oxygens. This leads to calculated barriers of θ_1 = 1469 cm^{-1} and θ_1 = 1680 cm^{-1} in *N*-ethyl maleimide and *N*-ethyl succinimide, respectively.

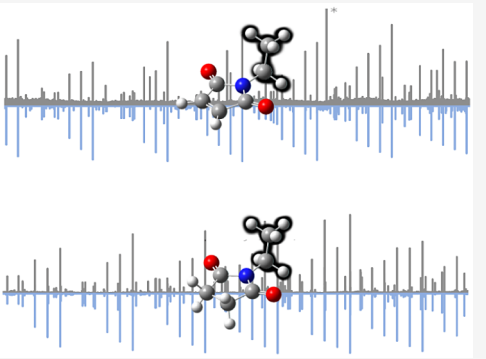

INTRODUCTION

Succinimides and maleimides are highly polar, 5-membered rings with an NH group surrounded by two adjacent C═O groups (Figure 1a,b). Both groups of molecules are important compounds in biological chemistry, biotechnology, and organic synthesis.[1−3] Succinimide and its derivatives are used pharmaceutically as analgesics[4] and anticonvulsants.[5−7] In industry, succinimides are also used as lubricants in oils, emulsion explosives, and corrosion inhibitors.[8] They also display antifungal and antimicrobial properties, and they even have activity as insecticides.[9] In these applications, substitution at the N atom is employed, making the structural consequences of *N*- substitution an important determiner of the overall molecular shape.

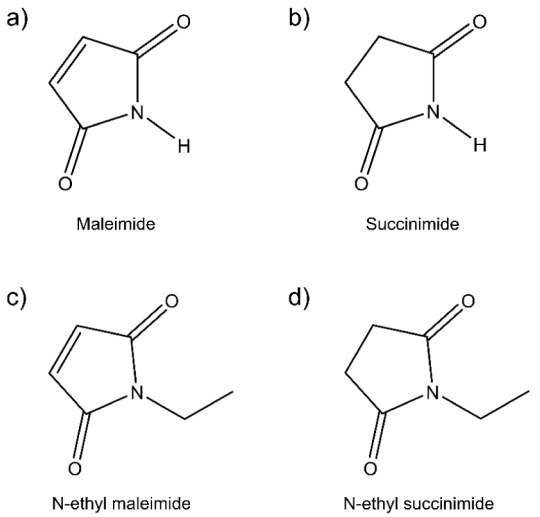

Figure 1. Chemical structures of a) maleimide, b) succinimide, c) *N*-ethyl maleimide, and d) *N*-ethyl succinimide.

In contrast to succinimides, the presence of a double bond in the ring makes maleimides an important class of building blocks in organic synthesis.[10,11] Maleimides are used in the protection of amino groups.[11] Fluorescent maleimide derivatives have been used to study the *in vivo* processes of intracellular trafficking, membrane association, and autotoxicity.[12] Considering the many uses of succinimide, maleimide, and their derivatives, these molecules have been the subject of a number of theoretical and spectroscopic studies, especially of their electronic and vibrational structure.[5,8,13−17]

Of the two parent molecules, maleimide and succinimide, only maleimide has been studied previously by microwave spectroscopy,[15] and no other rotationally resolved studies are available for these or any of their derivatives. The solid-state structure of maleimide has been measured by X-ray diffraction,[18] and the gas-phase structures of both maleimide

Received: April 9, 2024
Revised: June 27, 2024
Accepted: June 27, 2024
Published: July 9, 2024

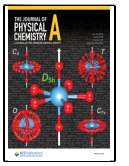

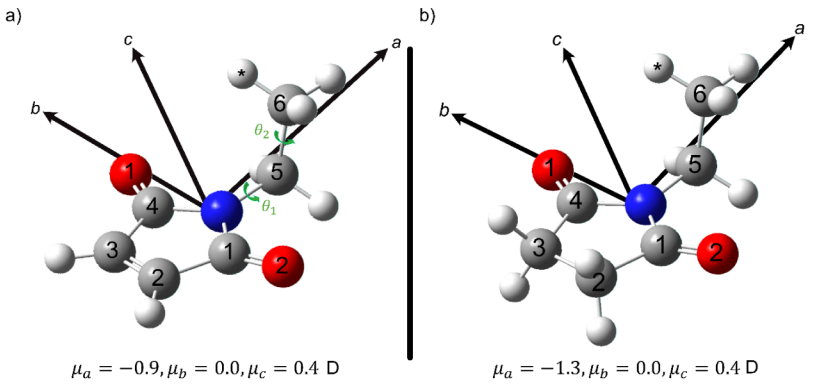

Figure 2. Optimized structures of a) *N*-ethyl maleimide (NEM) and b) *N*-ethyl succinimide (NES). The inertial axes are superimposed. The geometries were calculated at the B2PLYP-D3(BJ)/def2-TZVP level of theory. The dihedral angles are indicated by θ_1 = C(6)−C(5)−N−C(4) and θ_2 = N−C(5)−C(6)−H(*). The symmetry group of both molecules is C_{2v}.

and succinimide have been measured by electron diffraction.[19,20] To our knowledge, there are no previous studies of the rotational spectroscopy of *N*-ethyl-maleimide (NEM) or *N*-ethyl-succinimide (NES) in either the gas phase.

Microwave spectroscopy is a consummate "shape detector" for isolated molecules owing to its high resolution.[21−24] It can therefore provide critical structural details of these two molecules under gas-phase conditions in which intermolecular effects are absent, which is helpful for understanding the links between their structures and their chemical and biological properties.

In the present study, we focus on two alkyl derivatives, NEM and NES, shown in Figure 1c,d. We have recorded and analyzed their pure rotational spectra in the K_a band (26.5−40 GHz) with the help of density functional theory (DFT) calculations. In addition to providing a complete set of spectroscopic parameters for these species, the focus of the work is to determine the preferred orientation of the *N*-ethyl group on the five-membered rings of maleimide and succinimide.

QUANTUM CHEMICAL CALCULATIONS

Structure optimizations and harmonic vibrational frequency calculations were carried out on NEM and NES at several levels of theory using the Gaussian 16 program suite.[25] Important geometric and electronic structural parameters for all calculations are presented in Tables S.1 and S.2. The structures of NEM and NES were optimized using the B2PLYP[26] functional with the D3 dispersion correction and the Becke−Johnson damping function[27,28] with the def2-TZVP[29] basis set (Figure 2). We performed optimizations and subsequent anharmonic calculations at the B3LYP/6-311+G-(2d,p)[30−32] level of theory for both molecules, NEM and NES.

In order to explore the potential energy surface for the ethyl group, we carried out relaxed potential energy scans at the B2PLYP-D3(BJ)/def2-TZVP level of theory along two dihedral angles in both molecules. The scans were carried out in 36 steps of 10° each. The C(6)−C(5)−N−C(4) dihedral sets the orientation of the ethyl group relative to the plane of the ring; this scan determines if there is more than one conformational minimum for the ethyl group. The N−C(5)−C(6)−H(*) dihedral determines the methyl internal rotation barrier. Frequency calculations were performed at stationary points to confirm that true minima have no imaginary frequencies and that first order saddle points have only one imaginary frequency.

EXPERIMENTAL METHODS

Samples of NEM and NES were purchased (98%, Sigma-Aldrich) and used without further purification. The samples were loaded into a sample reservoir located directly before the pulsed valve, entrained in 3.75 bar of Ar, and were then introduced into the vacuum chamber held at 10^{-6} Torr using a pulsed (5 Hz) supersonic jet expansion. We used a pulsed valve (Parker General Valve, Series 9) with a pinhole of 1 mm diameter. Gas pulses of 650 μs duration were found to be optimal. To obtain sufficient vapor pressure, NEM was heated to 150 °C and NES was heated to 200 °C.

We used the K_a band (26.5−40 GHz) CP-FTMW spectrometer at UC Davis to investigate the rotational spectra. The details of the spectrometer have been previously described.[33] A chirped pulse is generated with a 16 GSa/s arbitrary waveform generator (AWG, Tektronix AWG70002A) coupled to an up-conversion bandwidth extension circuit to reach 26.5−40 GHz and amplified by a 170 W traveling wave tube amplifier (TWTA, Applied Systems Engineering 187 Ka-H). The chirp is broadcasted into the vacuum chamber through a 25 dBi horn antenna, and the molecular free induction decay (FID) is collected by a matching horn antenna. The FID is downconverted to 1−15 GHz and digitized at 50 GSa/s with a 16 GHz oscilloscope (Tektronix DSA71604C). The local oscillator and timing sources are referenced to a 10 MHz Rb clock (Stanford Research System, FS725), ensuring phase coherence. Each gas pulse was interrogated with 20 3 μs chirps each separated by 20 μs, yielding an effective acquisition rate of 100 FID/s at the repetition rate of 5 Hz. The total length of each FID was 11.65 μs.

RESULTS

The B2PLYP-D3(BJ)/def2TZVP optimized bond lengths and angles (Table S3) as well as the Cartesian coordinates for NEM and NES at all levels of theory are provided in the Supporting Information. The calculations predict that the 5-membered ring in both molecules is planar, with the ethyl group oriented out of the plane of the ring (Figure 2). From the calculations, we can observe that B2PLYP-D3(BJ)/def2TVZP is the level of theory with the lowest error when compared to the rotational constants and centrifugal distortion

https://doi.org/10.1021/acs.jpca.4c02330
J. Phys. Chem. A 2024, 128, 5541−5547

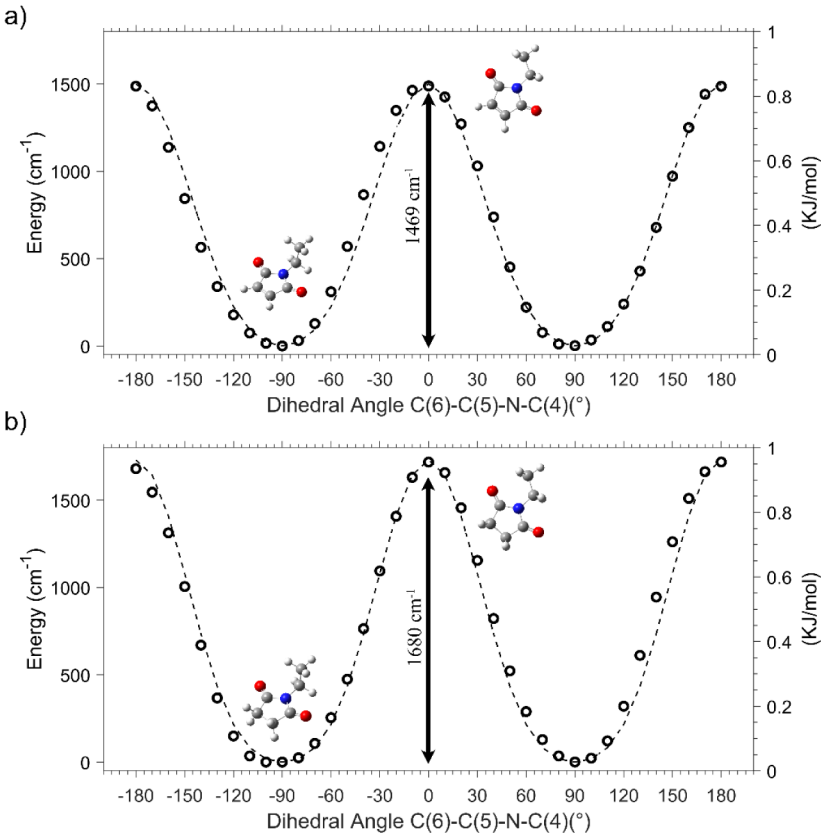

Figure 3. Relaxed potential energy curves of a) *N*-ethyl maleimide (NEM) and b) *N*-ethyl succinimide (NES) at the B2PLYP-D3(BJ)/def2-TZVP level of theory. These curves were calculated by rotating the dihedral angle C(6)−C(5)−N−C(4), which changes the orientation of the ethyl group relative to the plane of the ring. The double arrows indicate the barriers heights. The dashed lines are the fitted potentials to the relaxed potential energy using the functional form: $V(\theta) = \frac{1}{2}V_2(1 - \cos(2\theta)) + \frac{1}{2}V_4(1 - \cos(4\theta))$.

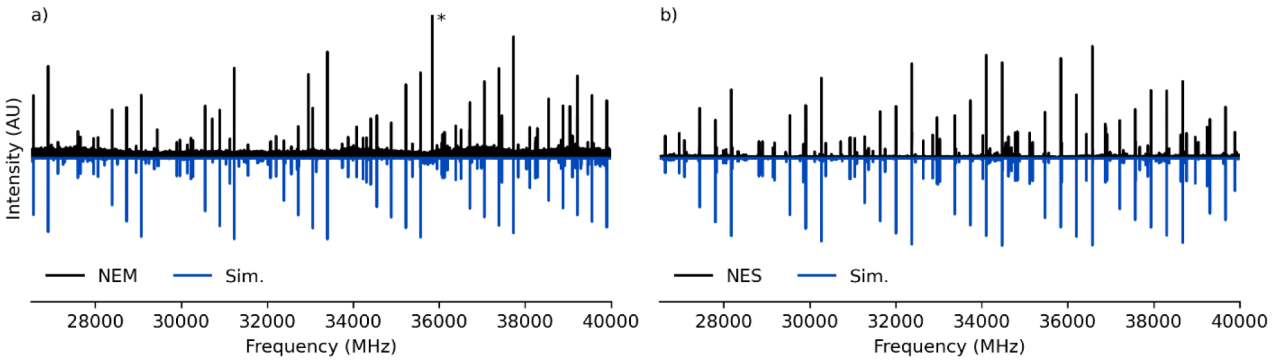

Figure 4. Experimental CP-FTMW rotational spectra of a) *N*-ethyl maleimide (NEM) and b) *N*-ethyl succinimide (NES) is shown in black. In blue, we show the best fit simulated spectrum at rotational temperature of 7.5 K for NEM and 9 K for NES. The experimental spectra of NEM and NES were averages of 200 k FIDs and 500 k FIDs, respectively. The asterisk indicates spurs lines.

constants for both NEM and NES. The error is lower than 0.15% for the rotational constants.

The results from the relaxed potential energy scan (PES) around the dihedral angle C(6)−C(5)−N−C(4) are shown in Figure 3. The calculations predict a single minimum at the perpendicular orientation for both molecules. The same behavior has been observed for ethylbenzene in which the heavy-atom planar conformation has been confirmed to be a first order saddle point.[34] Harmonic frequency calculations of the structure corresponding to the maximum of the PES scan likewise yielded a single imaginary frequency for both NEM and NES. The energy barriers were determined to be 1469 cm^{-1} for NEM and 1680 cm^{-1} for NES, respectively. While this potential is largely a 2-fold potential, the shape of the curve around the minima is widened while the barrier itself is narrower than a pure V_2 potential. As a result, we have fit the PES scans to V_2/V_4 potentials using the functional form $V(\theta) = \frac{1}{2}V_2(1 - \cos(2\theta)) + \frac{1}{2}V_4(1 - \cos(4\theta))$. The best-fit forms of this potential have significant V_4 terms, with the values for NEM (V_2 = 1490 ± 23 cm^{-1}, V_4 = −173 ± 24 cm^{-1}) somewhat smaller than those for NES (V_2 = 1704 ± 23 cm^{-1} and V_4 = −216 ± 24 cm^{-1}).

https://doi.org/10.1021/acs.jpca.4c02330
J. Phys. Chem. A 2024, 128, 5541−5547

The internal rotation of the methyl group was inspected by a second relaxed energy potential scan, yielding barriers of 1174 and 1169 cm^{-1} for NEM and NES, respectively. These are typical barriers for methyl rotation in an ethyl group.[35] Since these barriers are so high, splitting due to the methyl rotor is not expected to be observed in either of the experimental spectra, since the half-widths of the spectral lines are ∼80 kHz. To observe any splitting in our experimental spectra, the methyl barrier would need to be lower than 700−800 cm^{-1}.

Ethyl Maleimide. Figure 4a shows the acquired spectrum of NEM, which is characterized by a rotational temperature of about 7 K. Analysis of the spectrum was undertaken using PGOPHER.[36] Fits of the assigned quantum numbers were made utilizing a Watson A-reduced Hamiltonian in the I^r representation. Our fit included 65 rotational transitions with partial resolution of the nuclear hyperfine splittings due to the nitrogen nonzero nuclear spin, for a total of 142 unique frequencies. These transitions are primarily strong *a*-type lines along with a few weak *c*-type lines, assigned with a root-mean-square (RMS) deviation of 22.47 kHz between the observed and calculated frequencies. This is consistent with the calculated dipole moments μ_a = −0.9 D and μ_c = 0.4 D for NEM. The majority were R-branch transitions, some with distinctive patterns and others that lacked regular structure. The hyperfine splitting was in general collapsed over the range of *J* values observed (8−18), but it was possible to determine the χ_{aa} and $\chi_{bb} - \chi_{cc}$ quadrupole coupling tensor elements. Table 1 reports the asymmetry parameter κ to be 0.48 which indicates that NEM is highly asymmetric, nearly equally distant from the oblate and prolate top limits.

Table 1 presents the rotational constants, quartic centrifugal distortion constants, and nuclear quadrupole hyperfine coupling parameters that were determined for NEM. The table compares the experimental best-fit parameters with those calculated. For the rotational constants, we have adjusted our B2PLYP-D3(BJ)/def2-TZVP values by adding the difference from the A_e, B_e, and C_e rotational constants and the A_0, B_0, and C_0 rotational constants obtained from the anharmonic calculations obtained at B3LYP/6-311 + G(2d,p) level of theory. The agreement between the calculated and the experimental rotational constants is excellent (<0.09%). To convert the quartic distortion constants from the III^r representation reported in the Gaussian output[37] to the I^r representation, we used the τ centrifugal distortion constants from our anharmonic calculations. The agreement between the experimental quartic centrifugal distortion constants and calculated values is ∼15%, which is typical for these constants. The nuclear hyperfine coupling constants have a lower error between experiment and calculated values (>6%). All assigned transitions can be found in Table S4.

Table 1. Molecular Parameters for NEM Obtained from PGOPHER[a]

par.[b]	experimental	calculated[c]	% errors
A_0 [MHz]	2143.1988(29)	2145	0.09
B_0 [MHz]	1868.7333(22)	1870	0.08
C_0 [MHz]	1082.98458(36)	1084	0.09
Δ_J [kHz]	0.20300(84)	0.179	−13.4
Δ_{JK} [kHz]	4.4437(36)	3.849	−15.4
Δ_K [kHz]	−4.452(35)	−3.830	−16.2
δ_J [kHz]	0.06472(43)	0.058	−11.6
δ_K [kHz]	1.8465(58)	1.61	−14.7
χ_{aa} [MHz]	1.824(89)	1.71	−6.67
$\chi_{bb} - \chi_{cc}$ [MHz]	4.73(14)	4.73	0.00
μ_a [D]		−0.9	
μ_b [D]		0.0	
μ_c [D]		0.4	
RMS [kHz][d]	22.48		
κ[e]	0.48	0.48	
N_{lines}	142[f]		

[a]The experimental and calculated rotational constants, dipole moment components, distortion constants are reported. [b]All parameters refer to the principal axis system. A Watson A-reduced Hamiltonian in the I^r representation was used. [c]Calculated equilibrium rotational constants have been corrected for zero-point energy effects using anharmonic corrections (see text). [d]Microwave RMS is calculated with the following formula: $\sqrt{\sum[(\text{obs} - \text{calc})^2]/N}$. [e]Asymmetry parameter calculated with the following formula: $\kappa = \frac{2B - A - C}{A - C}$. [f]Unique frequencies.

Ethyl Succinimide. Figure 4b shows the 26.5−40 GHz rotational spectrum of NES. The rotational constants, quadrupole coupling constants, and centrifugal distortion constants were all determined from the 673 unique transitions (263 rotational transitions) using PGOPHER[36] based on a Watson A-reduced Hamiltonian in the I^r representation.

The majority of the observed transitions are *a*-type, as expected given the dipole moments (μ_a = −1.3, μ_b = 0.0, μ_c = 0.4). Similar to the NEM spectrum, clear strong patterns belonging to R-branches are present. The weaker transitions are a mix of *a*- and *c*-type transitions. By comparing the intensities of the transitions with the simulation, it was possible to estimate the rotational temperature to be 9 K. The fitted spectroscopic parameters and the calculated values are shown in Table 2; the total RMS deviation of the fit is 24.79 kHz. All assigned transitions can be found in Table S.5. The comparison between experiment and calculation for NES is of similar quality to that in NEM.

DISCUSSION

As previously stated, only *a*- and *c*-type transitions were observed for NEM and NES (Figure 4). Despite careful searches, no *b*-type transitions were observed. The presence of only *a*- and *c*-type transitions shows that the ethyl group is oriented perpendicular to the plane of the ring. In contrast to the parent molecules succinimide[20] and maleimide,[15] both of which have the N atom lying along the *b* axis, the mass of the ethyl group reorients the principal axes relative to the ring, leading to a strong μ_a component in the direction of the N atom and no μ_b component by symmetry. If instead the ethyl group were oriented in the plane of the ring, the spectrum would be *a*- and *b*-type, as μ_c would be 0 by symmetry.

The strongest lines in the NEM and NES spectra had signal/noise ratios of 60 and 200, respectively, which was not sufficient for detecting ^{13}C-substitued isotopologues in natural abundance. Isotopic substitution experiments would allow the heavy atom structure to be partially constrained experimentally. Nonetheless, the close correspondence between experimental rotational parameters and calculations lend confidence that the calculations have sufficient accuracy to use them in our structural assessment in what follows.

As shown in Figure 3, both molecules have a large energy barrier at the two equivalent planar orientations of the ethyl group arising primarily due to steric interactions with the two keto oxygens, along with contributions from loss of hyper-

https://doi.org/10.1021/acs.jpca.4c02330
J. Phys. Chem. A 2024, 128, 5541−5547

Table 2. Molecular Parameters for NES Obtained from PGOPHER[a]

par.[b]	experimental	calculated[c]	% errors
A_0 [MHz]	2061.47756(14)	2064	0.10
B_0 [MHz]	1791.73517(12)	1794	0.15
C_0 [MHz]	1050.31263(11)	1051	0.10
Δ_J [kHz]	0.14949(24)	0.135	−10.73
Δ_{JK} [kHz]	3.1721(10)	3.099	−2.36
Δ_K [kHz]	−3.1528(22)	−3.073	−2.60
δ_J [kHz]	0.04907(65)	0.044	−11.52
δ_K [kHz]	1.32251(62)	1.283	−3.08
χ_{aa} [MHz]	1.471(15)	1.41	−4.33
$\chi_{bb} - \chi_{cc}$ [MHz]	3.711(31)	3.52	−5.43
μ_a [D]	-	−1.3	-
μ_b [D]	-	0.0	-
μ_c [D]	-	0.4	-
RMS [kHz][d]	24.79	-	-
κ[e]	0.46	0.46	-
N_{lines}	263[f]	-	-

[a]The experimental and calculated rotational constants, dipole moment components, distortion constants are reported [b]All parameters refer to the principal axis system. A Watson A-reduced Hamiltonian in the I^r representation was used. [c]Calculated equilibrium rotational constants have been corrected for zero-point energy effects using anharmonic corrections (see text). [d]Microwave RMS is calculated with the following formula: $\sqrt{\sum[(\text{obs} - \text{calc})^2]/N}$. [e]Asymmetry parameter calculated with the following formula: $\kappa = \frac{2B - A - C}{A - C}$. [f]Unique frequencies.

conjugation between the imide group and alkyl chain and repulsion due to the eclipsing C−C−N−C interaction. Harmonic frequency calculations at the heavy atom planar maximum yielded only one imaginary frequency confirming it as a saddle point. We looked for evidence of steric strain at the transition states of the two molecules by comparing their structures with the optimized minimum energy structures. In its minimum energy structure with the ethyl group perpendicular to the plane, NEM (Figure 5a) has equivalent C(4)−N−C(5) bond angles that are 124.7°. However, for the transition state, the vertical plane of symmetry is lost and the two C−N−C(5) angles are distinct, 130.26°and 119.79°, with the larger angle on the same side as the ethyl group, as shown in Figure 5b. This structural adaptation reflects a significant repulsion between the same side keto oxygen and the ethyl group. Another significant change between these two structures is the O(1)−C(1)−N angle, which increases by almost 2° from the perpendicular structure (125.77°) to the planar one (127.72°). The N−C(5) bond length as well as some of the C−C bonds in the maleimide ring also experience small changes as shown in Table 3.

Similar structural changes upon internal rotation of the ethyl group in NES are observed despite the change from a double bond to a single bond in the ring. The perpendicular minimum energy structure has two equivalent C−N−C(5) angles of 123.15°, while for the transition state (planar conformation) the C−N−C(5) angle closer to the ethyl group increases to 129.09°, while its counterpart decreases to 118.06° (Figure 5d). As with NEM, the O(1)−C(1)−N angle also changes by ∼2° from the perpendicular structure (124.54°) to the planar one (126.54°). Even though NES has a single bond instead of a double bond in the ring, which could lead to less rigidity, the lengths of the C−C bonds in the ring do not seem to be more

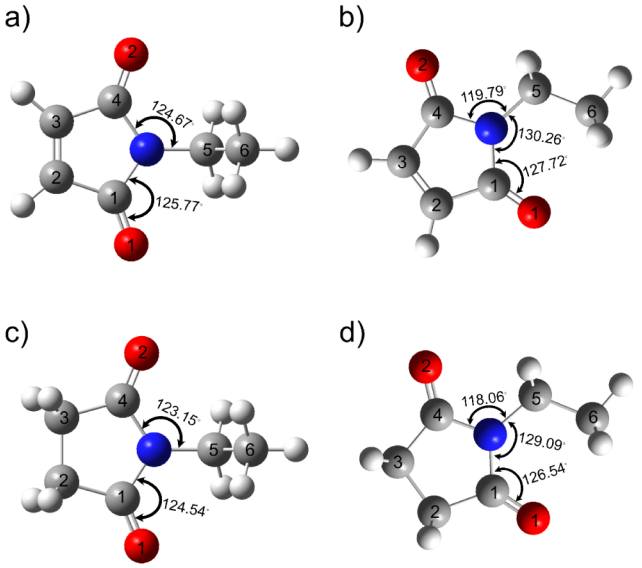

Figure 5. Summary of select angles in degrees for the ground and saddle point for NEM [a) and b)] and NES [c) and d)] that changed most between the two structures. The structures were optimized at the B2PLYP-D3(BJ)/def2TZVP level of theory.

Table 3. Calculated Distances and Angles for the Ground State and the Saddle Point of NEM and NES

	NEM		NES	
	minimum	saddle point	minimum	saddle point
C(1)−N−C(5)	124.67°	130.26°	123.15°	129.09°
C(4)−N−C(5)	124.67°	119.79°	123.15°	118.06°
O(1)−C(4)−N	125.77°	127.72°	124.54°	126.54°
C(1)−C(4) (Å)	2.29	2.29	2.32	2.32
C(1)−C(2) (Å)	1.50	1.51	1.52	1.52
C(2)−C(3) (Å)	1.33	1.33	1.53	1.52
C(3)−C(4) (Å)	1.50	1.49	1.52	1.51
C(4)−N (Å)	1.39	1.39	1.39	1.39
C(1)−N (Å)	1.39	1.39	1.39	1.40
N−C(5) (Å)	1.45	1.47	1.46	1.47
C(5)−O(1)	2.93	3.09	2.88	3.04
C(5)−O(2)		2.83		2.77
C(6)−O(1)	3.59	2.90	3.54	2.86
C(6)−O(2)		4.33		4.28

sensitive to the movement of the ethyl group in NES than for NEM (Table 3). The planarity of the ring in NES is retained through the entire ethyl rotation including at the transition state (Figure 5d).

CONCLUSION

The pure rotational spectra of NEM and NES were measured in the 26.5−40 GHz range with a CP-FTMW spectrometer, and all measured transitions were assigned for the first time, providing experimentally determined rotational, centrifugal distortion, and quadrupole coupling constants. The calculated parameters are in excellent agreement with the experimental values. To obtain a more complete and accurate gas phase structure and fit the bond lengths and angles, the ^{13}C, ^{18}O, and ^{15}N isotopologues will need to be measured. The presence of *c*-type transitions and absence of *b*-type transitions determined that the preferred orientation of the ethyl group in both molecules is perpendicular to the plane of their respective

https://doi.org/10.1021/acs.jpca.4c02330
J. Phys. Chem. A 2024, 128, 5541−5547

rings. Relaxed potential energy curves about the C(6)−C(5)−N−C(4) dihedral angle were calculated, providing barriers of 1469 and 1680 cm^{-1} for NEM and NES, respectively. These large barriers are a result of significant steric strain associated with the interaction of the ethyl group with the two carbonyl oxygens, leading to an increase in the C−N−C(5) bond angles by more than 5° at the transition state.

■ ASSOCIATED CONTENT

Supporting Information

The Supporting Information is available free of charge at https://pubs.acs.org/doi/10.1021/acs.jpca.4c02330.

Calculated rotational parameters and assigned transitions for NEM and NES (PDF)

Bond length and angles at B2PLYP/def2PVTZ level of theory for NEM and NES (ZIP)

Nuclear coordinates for NEM and NES and fit and original spectra for NEM and NES (ZIP)

■ AUTHOR INFORMATION

Corresponding Author

A. O. Hernandez-Castillo − *Department of Chemistry, Harvey Mudd College, Claremont, California 91711, United States;* orcid.org/0000-0001-7472-1044; Email: ahernandezcastillo@g.hmc.edu

Authors

Lughnasa York − *Department of Chemistry, Harvey Mudd College, Claremont, California 91711, United States*

Caroline Sorrells − *Department of Chemistry, Harvey Mudd College, Claremont, California 91711, United States;* orcid.org/0009-0004-3587-3909

Chisom A. Dim − *Department of Chemistry, University of California, Davis, Davis, California 95616, United States*

Kyle N. Crabtree − *Department of Chemistry, University of California, Davis, Davis, California 95616, United States;* orcid.org/0000-0001-5629-5192

Complete contact information is available at: https://pubs.acs.org/10.1021/acs.jpca.4c02330

Author Contributions

The manuscript was written through contributions of all authors. All authors have given approval to the final version of the manuscript.

Notes

The authors declare no competing financial interest.

■ ACKNOWLEDGMENTS

A.O.H.C. acknowledges start-up funds from Harvey Mudd College. K.N.C. acknowledges support from NSF grant AST-2042257. This work used Bridges-2 at Pittsburgh Supercomputing Center through allocation CHE220068 from the Advanced Cyberinfrastructure Coordination Ecosystem: Services & Support (ACCESS) program, which is supported by National Science Foundation grants #2138259, #2138286, #2138307, #2137603, and #2138296.

■ REFERENCES

(1) Baldwin, A. D.; Kiick, K. L. Tunable Degradation of Maleimide−Thiol Adducts in Reducing Environments. *Bioconjugate Chem.* **2011**, *22* (10), 1946−1953.

(2) Nardelli, F.; Paissoni, C.; Quilici, G.; Gori, A.; Traversari, C.; Valentinis, B.; Sacchi, A.; Corti, A.; Curnis, F.; Ghitti, M.; et al. Succinimide-Based Conjugates Improve IsoDGR Cyclopeptide Affinity to $\alpha_v\beta_3$ without Promoting Integrin Allosteric Activation. *J. Med. Chem.* **2018**, *61* (17), 7474−7485.

(3) Grassi, L.; Regl, C.; Wildner, S.; Gadermaier, G.; Huber, C. G.; Cabrele, C.; Schubert, M. Complete NMR Assignment of Succinimide and Its Detection and Quantification in Peptides and Intact Proteins. *Anal. Chem.* **2017**, *89* (22), 11962−11970.

(4) Obniska, J.; Sałat, K.; Librowski, T.; Kamiński, K.; Lipkowska, A.; Wiklik, B.; Rybka, S.; Rapacz, A. Antinociceptive Properties of N-Mannich Bases Derived from 3-Substituted Pyrrolidine-2,5-Dione in the Formalin Model of Persistent Pain in Mice. *Pharmacol Rep.* **2015**, *67* (1), 63−68.

(5) Vitnik, V. D.; Vitnik, Z. J.; Banjac, N. R.; Valentić, N. V.; Ušćumlić, G. S.; Juranić, I. O. Quantum Mechanical and Spectroscopic (FT-IR, 13C, 1H NMR and UV) Investigations of Potent Antiepileptic Drug 1-(4-Chloro-Phenyl)-3-Phenyl-Succinimide. *Spectrochim. Acta, Part A* **2014**, *117*, 42−53.

(6) Zhao, Z.; Yue, J.; Ji, X.; Nian, M.; Kang, K.; Qiao, H.; Zheng, X. Research Progress in Biological Activities of Succinimide Derivatives. *Bioorganic Chem.* **2021**, *108*, 104557.

(7) Wang, Y.; Bowman, J. M. *Ab Initio* Potential and Dipole Moment Surfaces for Water. II. Local-Monomer Calculations of the Infrared Spectra of Water Clusters. *J. Chem. Phys.* **2011**, *134* (15), 154510.

(8) Eşme, A.; Sagdinc, S. G. Conformational, Spectroscopic (FT-IR, FT-Raman, and UV-Vis), and Molecular Docking Studies of N-(2-Hydroxyethyl) Succinimide. *J. Mol. Struct.* **2019**, *1195*, 451−461.

(9) Fujinami, A.; Ozaki, T.; Nodera, K.; Tanaka, K. Studies on Biological Activity of Cyclic Imide Compounds: Part II. Antimicrobial Activity of l-Phenylpyrrolidine-2,5-Diones and Related Compounds. *Agric. Biol. Chem.* **1972**, *36* (2), 318−323.

(10) Thale, P. B.; Borase, P. N.; Shankarling, G. S. Magnetic Nanocatalyst for the Synthesis of Maleimide and Phthalimide Derivatives. *RSC Adv.* **2014**, *4* (103), 59454−59461.

(11) Osby, J. O.; Martin, M. G.; Ganem, B. An Exceptionally Mild Deprotection of Phthalimides. *Tetrahedron Lett.* **1984**, *25* (20), 2093−2096.

(12) Benkova, B.; Lozanov, V.; Ivanov, I. P.; Todorova, A.; Milanov, I.; Mitev, V. Determination of Plasma Aminothiols by High Performance Liquid Chromatography after Precolumn Derivatization with N-(2-Acridonyl)Maleimide. *J. Chromatogr. B* **2008**, *870* (1), 103−108.

(13) Krishnakumar, V.; Xavier, R. J.; Chithambarathanu, T. Density Functional Theory Study of Vibrational Spectra, and Assignment of Fundamental Vibrational Modes of Succinimide and N-Bromosuccinimide. *Spectrochim. Acta, Part A* **2005**, *62* (4−5), 931−939.

(14) Seliskar, C. J.; McGlynn, S. P. Electronic Spectroscopy of Maleimide and Its Isoelectronic Molecules. I. Maleimide and *N*-Alkylmaleimides. *J. Chem. Phys.* **1971**, *55* (9), 4337−4342.

(15) Pejlovas, A. M.; Oncer, O.; Kang, L.; Kukolich, S. G. Microwave Spectrum and Gas Phase Structure of Maleimide. *J. Mol. Spectrosc.* **2016**, *319*, 26−29.

(16) Woldbæk, T.; Klaboe, P.; Nielsen, C. J. The Vibrational Spectra of Maleimide and N-D Maleimide. *J. Mol. Struct.* **1975**, *27* (2), 283−301.

(17) Stamboliyska, B. A.; Binev, Y. I.; Radomirska, V. B.; Tsenov, J. A.; Juchnovski, I. N. IR Spectra and Structure of 2,5-Pyrrolidinedione (Succinimide) and of Its Nitranion: Experimental and Ab Initio MO Studies. *J. Mol. Struct.* **2000**, *516* (2−3), 237−245.

(18) Baltá-Calleja, F. J.; Ramos, J. G.; Barrales-Rienda, J. M. X-Ray Diffraction Study of Bulk Poly N-Substituted Maleimides. *Kolloid-Z. Z. Für Polym.* **1972**, *250* (5), 474−481.

(19) Harsányi, L.; Vajda, E.; Hargittai, I. The Molecular Structure of Maleimide: An Electron Diffraction Study. *J. Mol. Struct.* **1985**, *129* (3−4), 315−320.

(20) Vogt, N.; Khaikin, L. S.; Grikina, O. E.; Karasev, N. M.; Vogt, J.; Vilkov, L. V. Flexibility of the Saturated Five-Membered Ring in 2,5-Pyrrolidinedione (Succinimide): Electron Diffraction and Quan-

tum-Chemical Studies with Use of Vibrational Spectroscopy Data. *J. Phys. Chem. A* **2009**, *113* (5), 931−937.
(21) Brown, G. G.; Dian, B. C.; Douglass, K. O.; Geyer, S. M.; Shipman, S. T.; Pate, B. H. A Broadband Fourier Transform Microwave Spectrometer Based on Chirped Pulse Excitation. *Rev. Sci. Instrum.* **2008**, *79* (5), 053103.
(22) Gordy, W. Microwave Spectroscopy. *Rev. Mod. Phys.* **1948**, *20* (4), 668−717.
(23) Dicke, R. H.; Romer, R. H. Pulse Techniques in Microwave Spectroscopy. *Rev. Sci. Instrum.* **1955**, *26* (10), 915−928.
(24) Ekkers, J.; Flygare, W. H. Pulsed Microwave Fourier Transform Spectrometer. *Rev. Sci. Instrum.* **1976**, *47* (4), 448−454.
(25) Frisch, M. J.; Trucks, G. W.; Schlegel, H. B.; Scuseria, G. E.; Robb, M. A.; Cheeseman, J. R.; Scalmani, G.; Barone, V.; Petersson, G. A.; Nakatsuji, H., et al. *Gaussian 16, Revision C.01*, Gaussian Inc.: Wallingford CT, 2016.
(26) Grimme, S.; Neese, F. Double-Hybrid Density Functional Theory for Excited Electronic States of Molecules. *J. Chem. Phys.* **2007**, *127* (15), 154116.
(27) Grimme, S.; Ehrlich, S.; Goerigk, L. Effect of the Damping Function in Dispersion Corrected Density Functional Theory. *J. Comput. Chem.* **2011**, *32* (7), 1456−1465.
(28) Grimme, S.; Antony, J.; Ehrlich, S.; Krieg, H. A Consistent and Accurate *Ab Initio* Parametrization of Density Functional Dispersion Correction (DFT-D) for the 94 Elements H-Pu. *J. Chem. Phys.* **2010**, *132* (15), 154104.
(29) Weigend, F.; Ahlrichs, R. Balanced Basis Sets of Split Valence, Triple Zeta Valence and Quadruple Zeta Valence Quality for H to Rn: Design and Assessment of Accuracy. *Phys. Chem. Chem. Phys.* **2005**, *7* (18), 3297.
(30) Curtiss, L. A.; McGrath, M. P.; Blaudeau, J.-P.; Davis, N. E.; Binning, R. C.; Radom, L. Extension of Gaussian-2 Theory to Molecules Containing Third-Row Atoms Ga−Kr. *J. Chem. Phys.* **1995**, *103* (14), 6104−6113.
(31) McGrath, M. P.; Radom, L. Extension of Gaussian-1 (G1) Theory to Bromine-Containing Molecules. *J. Chem. Phys.* **1991**, *94* (1), 511−516.
(32) Becke, A. D. Density-Functional Thermochemistry III. The Role of Exact Exchange. *J. Chem. Phys.* **1993**, *98* (7), 5648−5652.
(33) Crabtree, K. N.; Westerfield, J. H.; Dim, C. A.; Meyer, K. S.; Johansen, S. L.; Buchanan, Z. S.; Stucky, P. A. Rotational Spectroscopy of Methyl Tert-Butyl Ether with a New Ka Band Chirped-Pulse Fourier Transform Microwave Spectrometer. *Phys. Chem. Chem. Phys.* **2024**, *26*, 13694−709.
(34) Caminati, W.; Damiani, D.; Corbelli, G.; Velino, B.; Bock, C. W. Microwave Spectrum and *Ab Initio* Calculations of Ethylbenzene: Potential Energy Surface of the Ethyl Group Torsion. *Mol. Phys.* **1991**, *74* (4), 885−895.
(35) Jelisavac, D.; Cortés Gómez, D. C.; Nguyen, H. V. L.; Sutikdja, L. W.; Stahl, W.; Kleiner, I. The Microwave Spectrum of the Trans Conformer of Ethyl Acetate. *J. Mol. Spectrosc.* **2009**, *257* (2), 111−115.
(36) Western, C. *PGOPHER Version 10.0*, University of Bristol, 2017. .
(37) Jean, D. R.; Wood, S. A.; Esselman, B. J.; Woods, R. C.; McMahon, R. J. Rotational Spectroscopy of 1-Cyano-2-Methylenecyclopropane (C_5H_5N)−A Newly Synthesized Pyridine Isomer. *J. Phys. Chem. A* **2024**, *128* (8), 1427−1437.

https://doi.org/10.1021/acs.jpca.4c02330
J. Phys. Chem. A 2024, 128, 5541−5547